



A single circularly permuted GFP sensor for inositol-1,3,4,5-tetrakisphosphate based on a split PH domain

Reiko Sakaguchi^a, Takashi Endoh^a, Seigo Yamamoto^a, Kazuki Tainaka^{a,b}, Kenji Sugimoto^a, Nobutaka Fujieda^c, Shigeki Kiyonaka^{d,e}, Yasuo Mori^{d,e}, Takashi Morii^{a,b,*}

^a Institute of Advanced Energy, Kyoto University, Uji, Kyoto 611-0011, Japan

^b CREST, JST, Uji, Kyoto 611-0011, Japan

^c Pioneering Research Unit for Next Generation, Kyoto University, Uji, Kyoto 611-0011, Japan

^d Department of Synthetic and Biological Chemistry, Graduate School of Engineering, Kyoto University, Katsura Campus, Nishikyo-ku, Kyoto 615-8510, Japan

^e CREST, JST, Katsura Campus, Nishikyo-ku, Kyoto 615-8510, Japan

ARTICLE INFO

Article history:

Received 8 July 2009

Revised 6 August 2009

Accepted 7 August 2009

Available online 13 August 2009

Keywords:

Biosensor

PH domain

Structure-based design

Green fluorescent protein

Inositol polyphosphates

ABSTRACT

A fluorescent sensor for the detection of inositol-1,3,4,5-tetrakisphosphate, Ins(1,3,4,5)P₄, was constructed from a split PH domain and a single circularly permuted GFP. A structure-based design was conducted to transduce a ligand-induced subtle structural perturbation of the split PH domain to an alteration in the population of the protonated and the deprotonated states of the GFP chromophore. Excitation of each distinct absorption band corresponding to the protonated or the deprotonated state of GFP resulted in an increase and a decrease, respectively, in the intensity of emission spectra upon addition of Ins(1,3,4,5)P₄ to the split PH domain-based sensor. The Ins(1,3,4,5)P₄ sensor retained the ligand affinity and the selectivity of the parent PH domain, and realized the ratiometric fluorescence detection of Ins(1,3,4,5)P₄.

© 2009 Elsevier Ltd. All rights reserved.

1. Introduction

A rational design of fluorescent biosensors for biologically relevant molecules in the cell would accelerate the ubiquitous application of the real-time fluorescent monitoring in the field of diagnosis and pharmacology. In order to visualize the bona fide behavior of target molecules, the genetically encoded biosensors based on green fluorescent protein (GFP) represent the attractive and practical strategy.^{1,2} Especially, the fluorescent resonance energy transfer (FRET) approach combined with two differently colored fluorescent proteins^{3–7} has been widely utilized for targeting the intracellular ions^{3,6,8–10} or small organic molecules such as cAMP.^{11–13} Because the FRET signal is effectively observed only when the distance separating the donor and the acceptor changes over a few nanometer, application of receptor proteins to the FRET biosensors is limited to those capable of undergoing large structural changes upon binding the substrate. As an alternative strategy, non-FRET biosensors based on a single circularly permuted (cp) GFP¹⁴ is also suitable for the development of versatile fluorescent biosensors that enable transducing the conformational change of the receptor associated

with the ligand binding event to a significant fluorescent response. In this case, the receptor protein is placed in the vicinity of the residues that would critically affect the photochemical property of the chromophore in GFP. Additionally, cpGFP mutants that retain their fluorescence property have been well investigated and been successfully converted into highly sensitive biosensors for intracellular calcium ion^{15,16} or cGMP.¹⁷ Nevertheless, the previously reported cpGFP biosensors have also taken advantage of rather major conformational changes of the receptor so as to output the sufficient fluorescence response. Therefore, manipulation of a sophisticated interplay between the small perturbation of the receptor conformation and the alteration of photochemical property of the GFP chromophore in the ligand binding event would provide a general design strategy for the fluorescent biosensor.

We have demonstrated the functional reconstitution strategy based on a split pleckstrin homology (PH) domain by dissecting the PH domain and tethering a coiled coil module to each subunit.¹⁸ The split PH domain designed from the PH domain of Phospholipase C δ_1 (PLC δ_1) folds into a functional structure when the split N-terminal and C-terminal halves are brought to close proximity. Furthermore, the reassembled split PH domain maintains binding selectively for *D*-myo-inositol-1,4,5-triphosphate, Ins(1,4,5)P₃, similar to that of the native PLC δ_1 PH domain. It is

* Corresponding author. Tel./fax: +81 774 38 3585.

E-mail address: t-morii@iae.kyoto-u.ac.jp (T. Morii).

possible that the dissection strategy of the split PH domain would permit the target binding region of the PH domain to be contiguously fused to the essential residue for the fluorescence behavior of the cpGFP chromophore without sacrificing the intrinsic function of parent cpGFP and PH domain.

We report here design and construction of a fluorescent sensor for an intracellular signal messenger *D*-myo-inositol-1,3,4,5-tetrakisphosphate, $\text{Ins}(1,3,4,5)\text{P}_4$, from a split PH domain of Bruton's tyrosine kinase (Btk)¹⁹ and a single cpGFP. The resulting split PH domain-cpGFP conjugate, Btk-cpGFP, exhibited bimodal absorption spectra corresponding to the protonated and deprotonated state of the chromophore in GFP. Addition of $\text{Ins}(1,3,4,5)\text{P}_4$ to Btk-cpGFP was accompanied by the decrease of 508 nm emission band by the excitation at 470 nm and the increase of the emission band by the excitation at 396 nm. As a result, the Btk-cpGFP realized the ratiometric fluorescence detection of $\text{Ins}(1,3,4,5)\text{P}_4$, and retained the ligand affinity and the selectivity of the original PH domain. Thus, the conformational change of the PH domain induced by the $\text{Ins}(1,3,4,5)\text{P}_4$ binding was transduced to the structural perturbation at the chromophore of conjugated GFP. The design strategy described here could be applied for other PH domains to construct gene-encoded fluorescent biosensors for biologically relevant ligands.

2. Results

2.1. Design of the cpGFP-fused split Btk PH domain

Wild-type GFP displays a pronounced bimodal absorption profile with two peaks around 400 and 470 nm, corresponding to the protonated and the deprotonated forms of the chromophore, respectively.²⁰ Although the unimodal fluorescence profile originating only from the singlet excited state of the deprotonated form is observed in the emission spectra of wild type GFP, the protonated form can also contribute substantially to the fluorescence emission via ultrafast proton transfer after excitation.^{21,22} It is generally accepted that the equilibrium between these forms in the ground state is governed by a hydrogen bond network that allows proton transfer between the chromophore and the side chains of neighboring amino acid residues. Especially, the configuration of Thr203 (residue numbers correspond to the wild type GFP throughout this work) and His148 residues against the chromophore appears to determine the protonated or deprotonated state of the chromophore from the crystal structure of wild-type GFP and S65T mutant.^{23,24} According to the previous report,¹⁴ cpGFP mutants with the novel termini introduced at His148 retained their fluorescent properties and yet were successfully converted

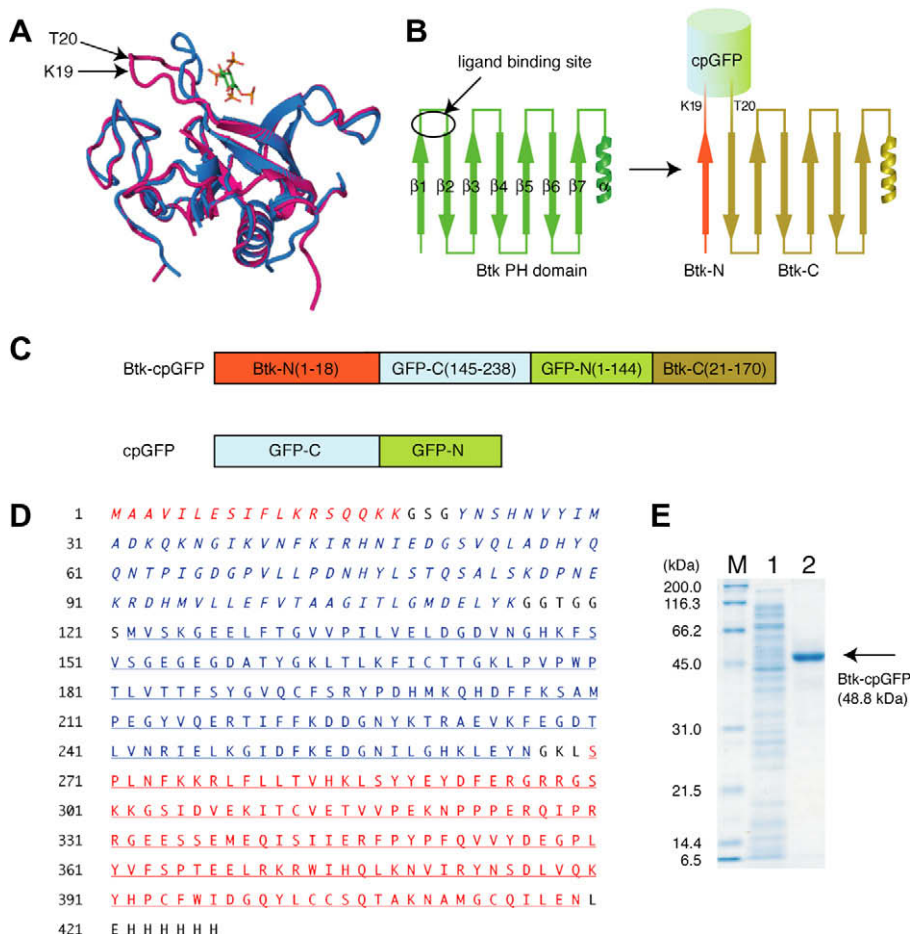


Figure 1. (A) The three dimensional structures reveal the slight structural alteration between the unliganded (magenta) and the $\text{Ins}(1,3,4,5)\text{P}_4$ -bound (blue) states of Btk PH domain [PDB ID; 1B55, 1BTK]. (B) Dissection strategy of Btk PH domain. Arrows represent the β -sheets of Btk PH domain (green), the Btk-N (orange) and Btk-C (ocher). The chromophore region cpGFP is fused precisely to the ligand $\text{Ins}(1,3,4,5)\text{P}_4$ binding site. (C) An illustration represents the construct of Btk-cpGFP. The cpGFP is sandwiched between the split halves of Btk PH domain. As a negative control, cpGFP without Btk PH domain was constructed. (D) An amino acid sequence of Btk-cpGFP. The original N-terminal (blue, underlined) and C-terminal (blue, italic) of GFP are swapped and flanked by the split halves (the N-terminal in red italic and the C-terminal in red underlined) of Btk PH domain with a linker region (black). (E) 12.5% SDS/polyacrylamide gel shows the CBB stained bands for the soluble fraction of *E. coli* lysate expressing Btk-cpGFP (lane 1) and purified Btk-cpGFP (lane 2). Protein markers are shown in lane M.

into highly sensitive fluorescent sensors. Thus, the split PH domain was fused to the Asn144–Tyr145 site of cpGFP so as to develop the ratiometric fluorescence sensor by the substrate binding-induced alteration of the protonation state of chromophore.

As for the receptor for $\text{Ins}(1,3,4,5)\text{P}_4$, a PH domain of Btk was chosen among the several candidates, due to the availability of the structural information for both the ligand-bound and the unbound states.^{25,26} Btk is categorized as Tec family kinase and possesses a PH domain²⁷ as a receptor of $\text{Ins}(1,3,4,5)\text{P}_4$, which induces its delicate conformational change (Fig. 1A).

In order to effectively transduce the modest structural disturbance of the PH domain accompanied by the $\text{Ins}(1,3,4,5)\text{P}_4$ binding event, the region to fuse GFP must be quite near the $\text{Ins}(1,3,4,5)\text{P}_4$ binding pocket of the Btk PH domain. Yet, the residues that directly interact with $\text{Ins}(1,3,4,5)\text{P}_4$ should not be altered to maintain the original selectivity and affinity. The amino acid residues located in the loop region (Fig. 1A), K19 and T20 (numbers correspond to the human Btk PH domain), were selected as the splitting point of the PH domain to insert the chromophore cpGFP (Fig. 1B). This mutant is designated as Btk-cpGFP (Fig. 1C and D). Additionally, cpGFP without the Btk PH domain was constructed as a negative control (Fig. 1C). The genes encoding above constructs were each cloned by PCR-based mutagenesis and expressed in *Escherichia coli*, followed by purification (Fig. 1E).

2.2. The optical properties of the Btk-cpGFP

We initially examined the UV/vis absorption spectra of Btk-cpGFP upon the addition of $\text{Ins}(1,3,4,5)\text{P}_4$ (Fig. 2A). In accordance with the case of native GFP, the absorption spectrum of Btk-cpGFP exhibited two distinct bands around 400 nm and 470 nm corresponding to the protonated and the deprotonated forms, respectively. The absorbance of the band at 400 nm increased in response to the increasing amount of $\text{Ins}(1,3,4,5)\text{P}_4$, while that of the band at 470 nm moderately decreased. These spectral changes could be ascribed to the $\text{Ins}(1,3,4,5)\text{P}_4$ binding event at the split PH

domain because no change in the absorption occurred upon addition of $\text{Ins}(1,3,4,5)\text{P}_4$ to cpGFP (Fig. 2B). Thus, it is quite likely that the $\text{Ins}(1,3,4,5)\text{P}_4$ binding shifts the ground-state equilibrium of the chromophore in Btk-cpGFP from the deprotonated state to the protonated state. Since both the absorption bands at 400 and 470 nm contributed to the fluorescence emission of GFP, such a population variation of the chromophore in the ground state would contribute to the ratiometric fluorescence sensing of the target $\text{Ins}(1,3,4,5)\text{P}_4$.

To evaluate the $\text{Ins}(1,3,4,5)\text{P}_4$ binding, the fluorescence spectra of Btk-cpGFP and cpGFP (200 nM) were recorded in the presence of $\text{Ins}(1,3,4,5)\text{P}_4$ at different excitation wavelengths (Fig. 3). In the case of Btk-cpGFP, the addition of $\text{Ins}(1,3,4,5)\text{P}_4$ resulted in the significant suppression of the emission intensity at 508 nm when excited at 470 nm. The emission intensity at 508 nm was slightly enhanced by the addition of $\text{Ins}(1,3,4,5)\text{P}_4$ when excited at 396 nm (Fig. 3B). On the other hand, the emission spectra of cpGFP excited neither at 470 nm nor 395 nm were affected by the addition of $\text{Ins}(1,3,4,5)\text{P}_4$ at all (Fig. 3C and D). The crystal structures of wild type GFP and S65T mutant demonstrated that the nitrogen atom of His 148 and the hydroxyl group of the chromophore are separated by a water molecule in the protonated form, but this nitrogen atom comes into contact with the hydroxyl group of the chromophore in the deprotonated form.^{23,24} Accordingly, perturbation of the His 148 residue detaching from the chromophore would result in the shift of the ground-state equilibrium from the deprotonated form to the protonated form. Comparison of the crystal structures of Btk PH domain between the $\text{Ins}(1,3,4,5)\text{P}_4$ -bound and unbound states (Fig. 1A) suggests that the $\text{Ins}(1,3,4,5)\text{P}_4$ binding event to loop 1 leads to perturbation at the β -strand 7 of cpGFP containing the His 148 residue. Such a structural change would induce the predominant formation of the protonated form in the ground state. Negative peaks at around 215 nm in the CD spectrum of Btk-cpGFP were slightly affected by the existence of $\text{Ins}(1,3,4,5)\text{P}_4$, confirming the delicate change in conformation (Fig. 3E). The emission ratio of 396-nm excitation versus 470-nm excitation in Btk-cpGFP showed a typical saturation behavior as in Figure 4, suggesting that the fluorescence change reflects the binding of $\text{Ins}(1,3,4,5)\text{P}_4$ to the Btk split PH domain. These results indicate that even the subtle structural perturbation of the Btk PH domain upon the ligand binding was sufficiently transduced into the ratiometric fluorescence response by the alteration of the ground-state equilibrium of the cpGFP chromophore.

2.3. Ratiometric detection of $\text{Ins}(1,3,4,5)\text{P}_4$

Similar ratiometric fluorescence titration experiments were conducted for other biologically relevant inositol phosphate derivatives to assess the selectivity of Btk-cpGFP and to compare with that of the parent Btk PH domain (Fig. 4). The wild type Btk PH domain possesses the highest affinity to $\text{Ins}(1,3,4,5)\text{P}_4$, and is capable of discriminating $\text{Ins}(1,3,4,5)\text{P}_4$ from $\text{Ins}(1,4,5)\text{P}_3$, in a highly specific manner.^{28,29}

The standard binding isotherm obtained from the ratiometric fluorescence response of Btk-cpGFP provided the dissociation constants (K_D) for $\text{Ins}(1,3,4,5)\text{P}_4$, $\text{Ins}(1,2,3,4,5,6)\text{P}_6$ and $\text{Ins}(1,4,5)\text{P}_3$ as 100 nM, 880 nM, and 136 μM , respectively (Table 1). Because these values are comparable with those reported for the parent Btk PH domain,^{28,29} cpGFP was successfully introduced into the vicinity of the $\text{Ins}(1,3,4,5)\text{P}_4$ binding site of the split Btk PH domain without sacrificing the intrinsic function of the original Btk PH domain.

3. Conclusion

We have constructed a fluorescent $\text{Ins}(1,3,4,5)\text{P}_4$ sensor by the structure-based design of a split PH domain conjugated to cpGFP.

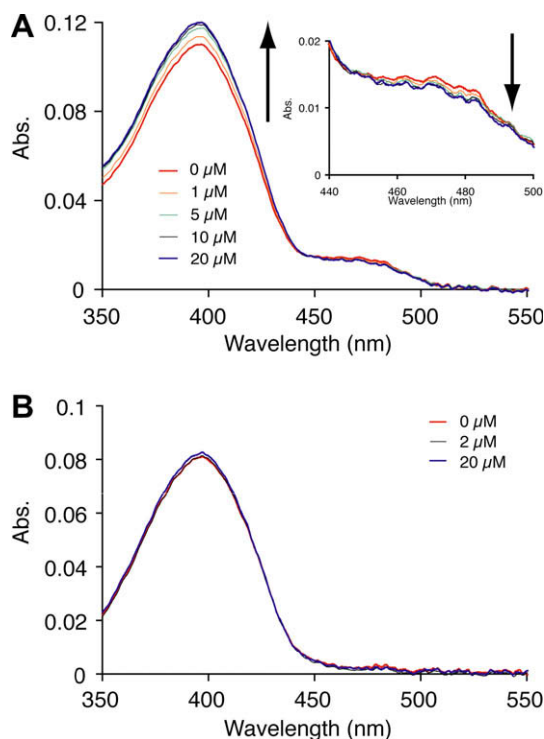


Figure 2. The UV–vis absorption spectral changes of (A) Btk-cpGFP and (B) cpGFP upon addition of $\text{Ins}(1,3,4,5)\text{P}_4$. A, inset, the absorption band around 470 nm of Btk-cpGFP decreased slightly upon addition of $\text{Ins}(1,3,4,5)\text{P}_4$.

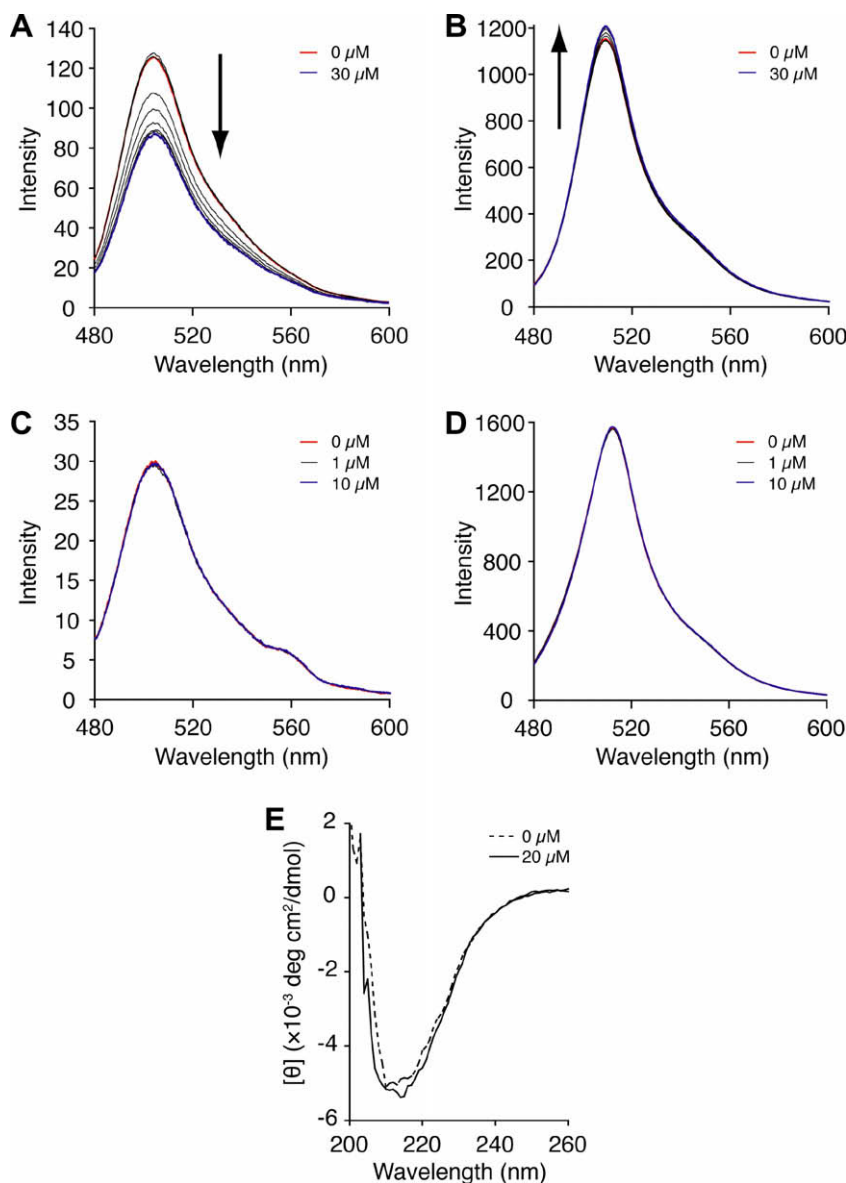


Figure 3. Fluorescence spectral changes of Btk-cpGFP (A; excited at 470 nm, B; excited at 396 nm) and the cpGFP (C; excited at 470 nm, D; excited at 395 nm) upon addition of Ins(1,3,4,5)P₄. (E) CD spectra of Btk-cpGFP under the absence (dashed) and presence (solid) of Ins(1,3,4,5)P₄ (20 μM).

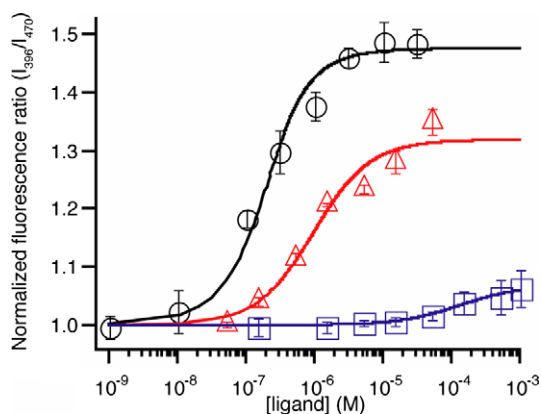


Figure 4. Fluorescent titration plots of the emission intensity ratio monitored at 508 nm (I_{396}/I_{470}) with excitation at two different wavelengths (396 and 470 nm) versus the concentration of inositol phosphate derivatives. The plot for the titration by Ins(1,3,4,5)P₄, Ins(1,4,5)P₃ and Ins(1,2,3,4,5,6)P₆ are shown in circles, squares and triangles, respectively.

Both Btk-cpGFP and cpGFP exhibited bimodal absorption spectra around 400 and 470 nm corresponding to the protonated and deprotonated state of the chromophore as observed for native GFP. In the case of Btk-cpGFP, addition of Ins(1,3,4,5)P₄ was accompanied by the increase in the intensity of the absorption band at 400 nm and the decrease of the band at 470 nm. Furthermore, the emission ratio of 396-nm excitation versus 470-nm excitation in Btk-cpGFP showed typical saturation behavior. Meanwhile, no change in the absorption and emission spectra was observed in cpGFP, supporting the hypothesis that the ground-state equilibrium between the protonated and deprotonated state of the chromophore was rationally regulated by the substrate binding at the split PH domain. The overall selectivity of the Btk-cpGFP against other inositol phosphates faithfully reflected that of the wild type Btk PH domain. Binding properties of the parent Btk PH domain are well retained in the designed split PH domain even after the fusion of the circular permuted GFP.

These results demonstrate that (1) the Ins(1,3,4,5)P₄-induced subtle conformational change of the Btk PH domain characterized

Table 1Dissociation constants (K_D) of Btk-cpGFP and the Btk PH domain to inositol phosphate derivatives

| Ligand | Btk-cpGFP K_D^a (μ M) | Btk PH domain K_D^b (μ M) |
|--------------------------------|------------------------------|----------------------------------|
| Ins(1,4,5)P ₃ | 136 \pm 16 | >10 |
| Ins(1,3,4,5)P ₄ | 0.10 \pm 0.02 | 0.057 \pm 0.003 |
| Ins(1,2,3,4,5,6)P ₆ | 0.88 \pm 0.18 | 0.83 \pm 0.02 |

^a Measured in 20 mM MOPS (pH 7.5), 150 mM NaCl, 3.0 mM DTT and 0.005% Tween 20 at 25 °C.^b From Refs. 28 and 29.

by the X-ray crystal analyses was preserved in the split PH domain configuration, and (2) the conformational change induced by the Ins(1,3,4,5)P₄ binding was transduced to the structural perturbation at the chromophore of conjugated cpGFP. Because the split PH domain derived from Btk PH domain precisely reflected the ligand selectivity of the original Btk PH domain, the design strategy described here could be applied for other PH domains. The native Btk PH domain as well as the Ins(1,3,4,5)P₄ sensor Btk-cpGFP display only a modest selectivity to Ins(1,3,4,5)P₄ against Ins(1,2,3,4,5,6)P₆. Further engineering of the ligand selectivity of Btk-cpGFP would realize in vivo application of this gene-encoded fluorescent Ins(1,3,4,5)P₄ sensor, which is currently underway in this laboratory.

4. Experimental

4.1. Materials

Inositol phosphate derivatives were purchased from Sigma (St. Louis, MO). Complete EDTA-free (protease inhibitor cocktail) was from Roche Applied Science (Mannheim, Germany). All the other reagents including the materials for the LB medium for culturing *E. coli* and buffers for chromatography were from Nacalai Tesque (Kyoto, Japan).

4.2. Methods

4.2.1. Plasmid constructs

cDNA encoding the PH domain of Btk (residues 1–170) was amplified with PCR from human spleen cDNA library (Clontech Laboratories, Mountain View, CA). DNA encoding wild type GFP was obtained by incorporating L64F and T65S mutations into the according region of pEGFP-C1 vector (Clontech Laboratories) by Quikchange® Site-Directed Mutagenesis Kit (Stratagene, La Jolla, CA). These DNAs were divided by PCR reaction using the primer encoding the respective scission site and a restriction enzyme site. The DNA pieces thus generated were ligated to obtained the full-length cpGFP-fused Btk mutants. These expression constructs were subcloned into pET29a (+) vector (Novagen, San Diego, CA).

4.2.2. Protein expression and purification

The plasmids were transformed into *E. coli* Rosetta™ cells (Invitrogen, Carlsbad, CA). Cells were grown at 37 °C until OD₆₀₀ reached 0.4, and protein expression was induced with 100 μ M IPTG for 20–24 h at 16 °C. The proteins were purified by His-tag affinity chromatography (HisTrap™ HP, GE Healthcare, Uppsala, Sweden), with a linear gradient of 20–500 mM imidazole in 20 mM CHES (pH 8.8), 500 mM NaCl, and 3.0 mM DTT. The fraction containing the GFP-derived absorption was collected and dialyzed against the initial condition of the next step. Additional purification was performed by HiTrap™ Q HP anion exchange column (GE Healthcare), with a linear gradient of 0.05–1 M NaCl in 20 mM EPPS (pH 8.2) with 3.0 mM DTT. Fractions containing mutated Btk-cpGFP were collected.

4.2.3. In vitro fluorescent measurements

Binding reactions of Btk-cpGFP with Ins(1,3,4,5)P₄, Ins(1,4,5)P₃ and Ins(1,2,3,4,5,6)P₆ were monitored with HITACHI F-7000 (HITACHI High-Tech, Tokyo, Japan) by measuring the changes in fluorescence emission that occurred upon addition of Ins(1,3,4,5)P₄ to a solution of 200 nM sensor dialyzed against 20 mM MOPS (pH 7.5), 150 mM NaCl, 3.0 mM DTT, 0.005% Tween 20 at 25 °C. Fluorescence emission spectra were recorded by addition of increasing amounts of InsP_n to saturation at the excitation wavelength at 396 and 470 nm, respectively. The dissociation constant of the complex of Btk-cpGFP and InsP_n was determined by measuring the change in the ratio of fluorescence emission at 508 nm for each excitation wavelength. The results were fit to the binding isotherm,

$$F = 1 + (F_{\max} - 1) * K_D + [\text{InsP}_n] + C - ([\text{InsP}_n]^2 + 2K_D[\text{InsP}_n] - 2C[\text{InsP}_n] + 2CK_D + C + K_D^2)^{1/2} / 2C \quad (1)$$

where F is the normalized fluorescence ratio (I_{396}/I_{470}), F_{\max} is the relative fluorescence ratio at saturation, K_D is the dissociation constant, C is the concentration of the sensor (200 nM) and $[\text{InsP}_n]$ is the concentration of Ins(1,3,4,5)P₄ or other inositol phosphate derivatives in selectivity assays.

4.2.4. CD spectrum measurement

The changes in CD spectra that occurred upon addition of Ins(1,3,4,5)P₄ to a solution of sensor Btk-cpGFP (4 μ M) were obtained with J-725 CD spectrometer (Jasco, Tokyo, Japan) by using a 1-mm cell at 25 °C. The conditions were 20 mM MOPS (pH 7.5), 150 mM NaCl, 3.0 mM DTT, 0.005% Tween 20, and the spectra were average of 64 scans.

Acknowledgments

This work was supported in part by the Grants-in-Aid for Scientific Research from the Ministry of Education, Culture, Sports, Science and Technology, Japan to T.M. (Nos. 19021023, 20241051).

References and notes

1. Tsien, R. Y. *Annu. Rev. Biochem.* **1998**, 67, 509.
2. Remington, S. J. *Curr. Opin. Struct. Biol.* **2006**, 16, 714.
3. Miyawaki, A.; Llopis, J.; Heim, R.; McCaffery, J. M.; Adams, J. A.; Ikura, M.; Tsien, R. Y. *Nature* **1997**, 388, 882.
4. Truong, K.; Ikura, M. *Curr. Opin. Struct. Biol.* **2001**, 11, 573.
5. Souslova, E. A.; Chudakov, D. M. *Biochemistry (Mosc)* **2007**, 72, 683.
6. Nagai, T.; Ibatani, K.; Park, E. S.; Kubota, M.; Mikoshiba, K.; Miyawaki, A. *Nat. Biotechnol.* **2002**, 20, 87.
7. Rizzo, M. A.; Springer, G. H.; Granada, B.; Piston, D. W. *Nat. Biotechnol.* **2004**, 22, 445.
8. Miyawaki, A.; Griesbeck, O.; Heim, R.; Tsien, R. Y. *Proc. Natl. Acad. Sci. U.S.A.* **1999**, 96, 2135.
9. Truong, K.; Sawano, A.; Mizuno, H.; Hama, H.; Tong, K. I.; Mal, T. K.; Miyawaki, A.; Ikura, M. *Nat. Struct. Biol.* **2001**, 8, 1069.
10. Mizuno, H.; Sawano, A.; Eli, P.; Hama, H.; Miyawaki, A. *Biochemistry* **2001**, 40, 2502.
11. Zaccaro, M.; Pozzan, T. *Science* **2002**, 295, 1711.
12. Sato, M.; Hida, N.; Ozawa, T.; Umezawa, Y. *Anal. Chem.* **2000**, 72, 5918.
13. Honda, A.; Adams, S. R.; Sawyer, C. L.; Lev-Ram, V.; Tsien, R. Y.; Dostmann, W. R. *Proc. Natl. Acad. Sci. U.S.A.* **2001**, 98, 2437.
14. Baird, G. S.; Zacharias, D. A.; Tsien, R. Y. *Proc. Natl. Acad. Sci. U.S.A.* **1999**, 96, 11241.
15. Nakai, J.; Ohkura, M.; Imoto, K. *Nat. Biotechnol.* **2001**, 19, 137.
16. Nagai, T.; Sawano, A.; Park, E. S.; Miyawaki, A. *Proc. Natl. Acad. Sci. U.S.A.* **2001**, 98, 3197.
17. Nausch, L. W.; Ledoux, J.; Bonev, A. D.; Nelson, M. T.; Dostmann, W. R. *Proc. Natl. Acad. Sci. U.S.A.* **2008**, 105, 365.
18. Sugimoto, K.; Mori, Y.; Makino, K.; Ohkubo, K.; Morii, T. *J. Am. Chem. Soc.* **2003**, 125, 5000.
19. Fukuda, M.; Kojima, T.; Kabayama, H.; Mikoshiba, K. *J. Biol. Chem.* **1996**, 271, 30303.

20. Morise, H.; Shimomura, O.; Johnson, F. H.; Winant, J. *Biochemistry* **1974**, *13*, 2656.
21. Chatteraj, M.; King, B. A.; Bublitz, G. U.; Boxer, S. G. *Proc. Natl. Acad. Sci. U.S.A.* **1996**, *93*, 8362.
22. Kennis, J. T.; Larsen, D. S.; van Stokkum, I. H.; Vengris, M.; van Thor, J. J.; van Grondelle, R. *Proc. Natl. Acad. Sci. U.S.A.* **2004**, *101*, 17988.
23. Ormo, M.; Cubitt, A. B.; Kallio, K.; Gross, L. A.; Tsien, R. Y.; Remington, S. J. *Science* **1996**, *273*, 1392.
24. Brejc, K.; Sixma, T. K.; Kitts, P. A.; Kain, S. R.; Tsien, R. Y.; Ormo, M.; Remington, S. J. *Proc. Natl. Acad. Sci. U.S.A.* **1997**, *94*, 2306.
25. Baraldi, E.; Djinnovic Carugo, K.; Hyvonen, M.; Surdo, P. L.; Riley, A. M.; Potter, B. V.; O'Brien, R.; Ladbury, J. E.; Saraste, M. *Structure* **1999**, *7*, 449.
26. Hyvonen, M.; Saraste, M. *EMBO J.* **1997**, *16*, 3396.
27. Mohamed, A. J.; Yu, L.; Backesjo, C. M.; Vargas, L.; Faryal, R.; Aints, A.; Christensson, B.; Berglof, A.; Vihinen, M.; Nore, B. F.; Smith, C. I. *Immunol. Rev.* **2009**, *228*, 58.
28. Cozier, G.; Sessions, R.; Bottomley, J. R.; Reynolds, J. S.; Cullen, P. J. *Biochem. J.* **2000**, *349*, 333.
29. Kojima, T.; Fukuda, M.; Watanabe, Y.; Hamazato, F.; Mikoshiba, K. *Biochem. Biophys. Res. Commun.* **1997**, *236*, 333.